An Artificial Neural Network Approach for Optical-SAR Imagery Fusion and Landslide Mapping

Yi-Keng Chen[1], Shou-Hao Chiang[1], Chung-Pai, Chang[1]

[1]Center for Space and Remote Sensing Research, National Central University,
No. 300, Zhongda Rd., Zhongli District, Taoyuan City 32001, Taiwan,
d163172121@gmail.com, gilbert@csrsr.ncu.edu.tw, cpchang@csrsr.ncu.edu.tw

KEYWORDS: landslide, image fusion, ANN, NDSI, NDVI

ABSTRACT: In the mountainous areas of Taiwan, affected by active tectonics, frequent typhoons and human activities, landslides are commonly induced by heavy rainfalls especially during typhoon seasons. During Typhoon Morakot (2009), the heavy rainfall induced large-scale landslide and caused severe damages in the mountainous region. This study focuses on landslide detection in Laonong River watershed in southern Taiwan. Image fusion can visually or statistically enhance the characteristics of land-objects. Usually, investigators mainly detect bare surface of landslides by using optical images instead of using synthetic aperture radar (SAR) images to identify the erosion, transportation and deposition patterns, which can be critical to landslide susceptibility assessment. Thus, this study aims to develop an Optical-SAR image fusion for an advanced landslide mapping task. In this study, SAR data is used to detect the change of land surface by distinguishing backscatters of images before and after the Typhoon event. In addition, the machine-learning method, artificial neural network (ANN), was operated for landslide pattern fusion and mapping practice. With applying image segmentation, Normalized Difference Sigma-naught Index (NDSI) from SAR images and Normalized Difference Vegetation Index difference ($NDVI_{diff}$) from optical images were generated, and calculated their texture statistics, such as mean, standard deviation, contrast, entropy, homogeneity and dissimilarity. Landslide detection results were assessed by overall accuracy (OA) and kappa coefficient, with comparing to a manually interpreted landslide inventory. Result shows the OA of optical-SAR image fusion is 0.896 and the kappa coefficient is 0.547, which has better performance than results with only using optical or SAR images for landslide detection.

1. INTRODUCTION

Landslide is one of common natural hazards in mountainous area in Taiwan. It causes not only considerable loss of property and life but also environmental problems such as soil and slope erosion. Typhoon Morakot was a catastrophic typhoon to impact Taiwan in August, 2009. The landslide disaster resulted in more than six-hundred and missing people. It is necessary and critical to detect event-landslides and monitor their mobility such as reactivation and sediment regeneration. By using machine learning methods and analyzing landslide textures from satellite images, it can help researchers to detect landslide area and generate landslide inventory rapidly and accurately right after a typhoon event.

2. STUDY AREA

The study area is a portion of Laonong River watershed, locates at Kaohsiung City, Taiwan. The region is characterized by sub-tropic monsoon climate. The rainy season is characterized by plum rain season and typhoons from May to September. The annual rainfall is about 1500 to 2000 mm. The elevation of the region is from 257 to 1673 m. Terrains are rugged and the altitude difference is more than 1000 m. Thus, in this area, landslides are commonly induced during typhoon seasons. During the incursion of Typhoon Morakot (2009), the heavy rainfall created large-scale landslides and debris flows and caused severe damages in the study area (Fig. 1).

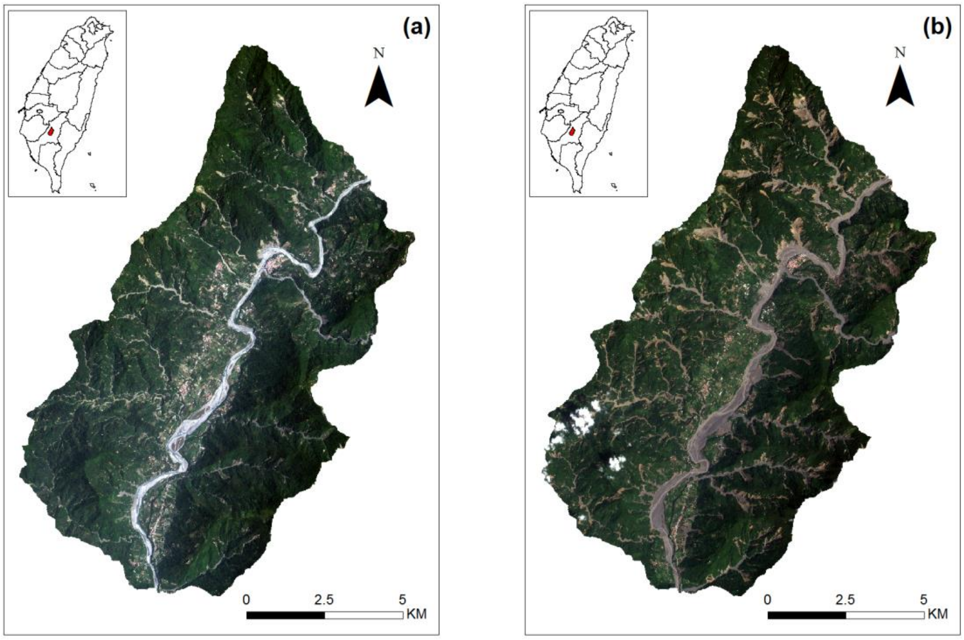

Fig 1. Formosat-2 image of study area. (a) The Formosat-2 image (2009.05.09) taken before Typhoon Morakot. (b) The Formosat-2 image (2009.09.12) taken after Typhoon Morakot. Typhoon Morakot (2009) caused considerable landslides and debris flows.

3. DATA

This research used optical images and SAR images for image fusion and landslide detection. For optical images, two FORMOSAT-2 images, taken on May 9 (pre-event image) and September 12 (post-event image), 2009, were collected. The spatial resolution of FORMOSAT-2 is 8 m, and the Normalized Difference Vegetation Index difference ($NDVI_{diff}$) were calculated for landslide detection. For SAR images, ALOS-PALSAR products, HH polarization images of fine mode, were chosen. The spatial resolution of SAR images used in this study is also 8 m. Two ALOS images, acquired on July 8 (pre-event) and August 23 (post-event), 2009, were used to analyze the change of backscattering before and after Typhoon Mprakot. The index NDSI (Normalized Difference Sigma-naught Index, NDSI) was calculated for this purpose and will be introduced in following section.

4. METHODS

4.1 Normalized Difference Vegetation Index difference ($\mathbf{NDVI_{diff}}$)

Normalized Difference Vegetation Index (NDVI) considers the deviation between Near-Infrared (NIR) and Red band, which can be used to determine the density of green on a patch of land. For landslide detection in forest area, due to the conversion from vegetated land to bare-soil, the change of NDVI before and after a landslide event can be significant. In this study, NDVI images pre and post-Typhoon Morakot, were used to calculated $NDVI_{diff}$ for landslide detection. $NDVI_{diff}$ value takes from -2 to 2. The equation shows as follows:

$$\mathrm{NDVI_{diff}} = \left(\frac{\mathrm{NIR} - \mathrm{Red}}{\mathrm{NIR} + \mathrm{Red}}\right)_{0912} - \left(\frac{\mathrm{NIR} - \mathrm{Red}}{\mathrm{NIR} + \mathrm{Red}}\right)_{0509}$$

where 0912 is NDVI value acquired in September 12, and 0509 is NDVI value acquired in May 12.

4.2 Normalized Difference Sigma-naught Index (NDSI)

Normalized Difference Sigma-naught Index (NDSI) derives normalized different value of sigma-naught value between two SAR images. The master image value subtract the slave image value divided the sum of master image value and the slave image value. It ranges from -1 to 1. In this study, the image of August 23 was selected as master image and the image of July 8 was selected as slave image. The equation shows as follows:

$$\mathrm{NDSI} = \frac{\sigma_0^{\mathrm{master}} - \sigma_0^{\mathrm{slave}}}{\sigma_0^{\mathrm{master}} + \sigma_0^{\mathrm{slave}}}$$

where σ_0 is backscatter coefficient which represents the radar signal intensity (dB).

4.3 Image Segmentation

The aim of image segmentation is to extract texture characteristics which can contribute to landslide detection. Both NDSI and $NDVI_{diff}$ results were separated in numerous segments by calculating their mean pixel value, and each segment has several pixels. The segmentation process was visually conducted by trial and error until the best segment size was found. In this study, 6 texture images, including mean, standard deviation, contrast, entropy, homogeneity and dissimilarity were extracted from NDSI and $NDVI_{diff}$, and used in the machine learning classification.

4.4 Artificial Neural Network (ANN)

In this study, Feed-forward Neural Network (FNN) method was tested to generate the classification result. It is the first and simplest type of artificial neural network (ANN). In this network, the information moves in only one direction and forward from the input nodes, through the hidden nodes and to the output nodes. There are no cycles or loops in the network. In the training process, 6 variables for NDSI and 6 variables for $NDVI_{diff}$ texture images (totally 12 variables) were imported as the input layer. By randomly selecting 1000 landslide and 1000 non-landslide points as the training data, the FNN looped 1000 times to develop the optimal model for landslide detection. In this study, three ANN models are derived: they are models trained by (1) 6 NDSI texture images, (2) 6

NDVI$_{diff}$ texture images and (3) 12 images from NDSI and NDVI$_{diff}$. The third model was considered suitable for optical-SAR image fusion.

4.5 Accuracy Assessment

In this study, three ANN results (as mentioned above) were compared with ground truth for accuracy assessment. The overall accuracy and kappa coefficient were calculated to assess the mapping accuracy. The ground truth also used to examine the strength and weakness of SAR derived and optical derived landslide mapping result.

5. RESULTS AND DISCUSSION

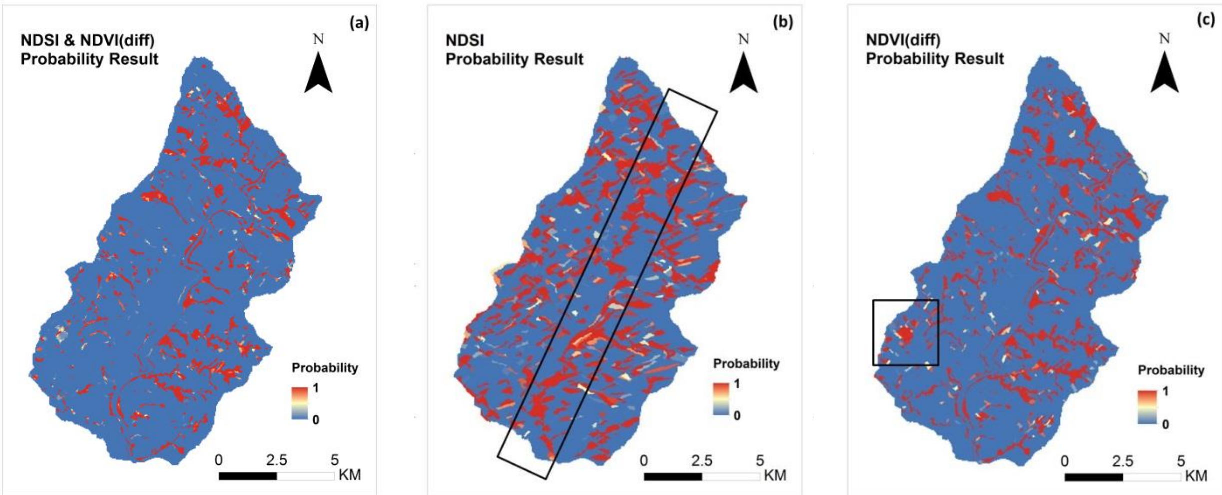

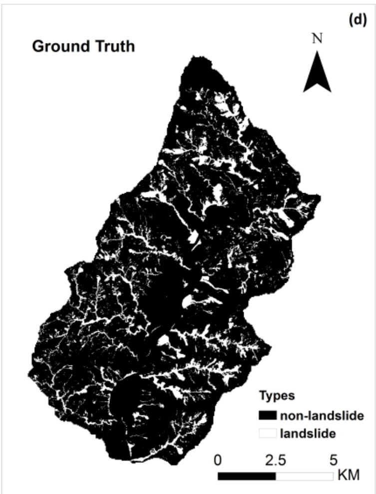

Fig 2. Landslide detection results (in probability) and landslide inventory (binary ground truth). (a) Landslide detection result generated from optical-SAR fused data. (b) Landslide detection result generated from only NDSI texture images. The rectangular box indicates that ANN classified the river channel as landslide area in SAR images. (c) Landslide detection result generated from only NDVI$_{diff}$ texture images. The square box indicates that ANN classified the cloud coverage in as landslide area. (d) The binary landslide inventory (ground truth) map, which was manually interpreted aerial photos right after the Typhoon Morakot event.

The classification results show landslide probability derived from three models: (1) 12 images from optical-SAR fusion, (2) 6 optical texture images and (3) 6 SAR texture images (Fig 2 a, b and c). This study uses probability threshold -0.5 to produce the final landslide detection results (binary) from probability maps. Comparing with a binary landslide inventory (Fig 2. d), we can calculate the overall accuracy and kappa coefficients of optical-SAR image fusion which are 0.896 and 0.547 respectively (Table 1). For landslide detection with using only SAR and only optical data, OAs and kappa coefficients are 0.703, 0.885 and 0.108, 0.556 respectively (Table 1). In the NDSI probability map (Fig 2. b), ANN model classified the river channel in the square box as landslide area because their textures in radar images are similar. In $NDVI_{diff}$ probability map (Fig 2. c), ANN model classified the cloud area in the square box as landslide area because of their similar $NDVI_{diff}$ values. These two kinds of misjudgment resulted in lower OA and kappa coefficient.

For landslide detection, the OA and kappa coefficient results from image fusion and optical images are higher than SAR images. Because some geometric deformations like fore shortening, layover and shadow would appear in the rugged area or highly relief terrain, so the radar signal would be masked or missing, and could be also projected and interpolated onto the surface. These reasons resulted in some distortion and deviation in a NDSI image (Fig 2. b), and lead to considerable misclassification of landslide.

Table 1. Results of the landslide classification accuracy assessment.

Variables	Overall Accuracy (OA)	Kappa coefficient
NDSI & $NDVI_{diff}$	0.896	0.547
NDSI	0.703	0.108
$NDVI_{diff}$	0.885	0.556

6. CONCLUSION

This study extracts NDSI textures from ALOS-1 imagery and $NDVI_{diff}$ textures from Formosat-2 imagery. An experimental threshold 0.5 of landslide probability was used to classify the landslide and non-landslide area. The better landslide detection result were obtained, indicating the applicability of optical-SAR image fusion method and artificial neural network for landslide detection in the study area. However, SAR texture images have lower contribution to mapping accuracy than optical texture images. The main reason is the considerable deviation between SAR images and optical images because of the lack of effective radar signal. As optical and SAR images could not be coregistered well over the slope surface, the classification accuracy would be lower.

REFERENCE

Chiang, J., Cheng, K., Chen, K. (2005). Landcover classification using multi-sensor images. Journal of Chinese Agricultural Engineering Vol.51, No. 4, (2005) 84-96.

Wang, L., Sawada, K. (2007). Fusion of SPOT and SAR images for land cover classification. Journal of Photogrammetry and Remote Sensing (2007) 59-72.

Wu, M., Chen, K. , Moriguchi, S. (2013). Landslide susceptibility analysis with logistic regression model based on FCM sampling strategy. Computer & Geoscience 57 (2013) 81-92.

Ventisette, C., Righini, G., Moretti, S., Casagli, N. (2014). Multitemporal landslides inventory map updating using spaceborne SAR analysis. International Journal of Applied Earth Observation and Geoinformation 30 (2014) 238-246.

Chen, C. W., Saito, H., Oguchi, T. (2015). Rainfall intensity–duration conditions for mass movements in Taiwan. Progress in Earth and Planetary Science (2015)2:14.